Turkish Journal of Electrical Engineering & Computer Sciences

http://journals.tubitak.gov.tr/elektrik/

Research Article

Turk J Elec Eng & Comp Sci
(2017) 25: 4854 – 4866

doi:10.3906/elk-1701-93

On the design of equal division single-band filtering dividers with an extended transmission line and resistor as isolation elements

Zafar Bedar KHAN*, Huiling ZHAO
Department of Electronics and Information, Northwestern Polytechnical University, Xian, P.R. China

Received: 09.01.2017 • **Accepted/Published Online:** 13.07.2017 • **Final Version:** 03.12.2017

Abstract: This paper introduces a new scheme for effective output port isolation and return loss in RF-filtering divider design. The proposed design incorporates an extended transmission line and a conventional resistor as isolation elements. The technique has a simpler microstrip circuit implementation when it comes to the integration of a single-band band-pass filter with a Wilkinson power divider to achieve simultaneous filtering–dividing action. It is established that if a band-pass filter with a certain fractional-bandwidth is matched to 70.7 Ω, a transmission line section and isolation resistor are sufficient for achieving reasonable output port return loss and isolation in the resulting filtering divider. In experimental validation, two single-band band-pass filters, namely a coupled-line filter and an open-loop coupled resonator triangular filter with center frequencies of 3 GHz and 1 GHz, respectively, effectively replace the conventional quarter-wavelength transformers for equal division of power. The proposed filtering divider structures were fabricated and a reasonable agreement was observed between respective simulated and measured S-parameter responses. The experimental results for a coupled-line filtering power divider and an open-loop triangular filtering power divider were as follows: 1 dB fractional-bandwidths of 15.3% and 12%, port isolations better than 31 dB and 20 dB, and good out-of-band performances up to $2.67f_0$ and $2.85f_0$, respectively.

Key words: Coupled line filter, open loop coupled triangular filter, band-pass filter, filtering divider, equal split

1. Introduction

Vital to most microwave/RF front ends for signal selectivity and equal/unequal power division, respectively, passive band-pass filter (BPF) and power dividers (PD) cause high insertion loss (IL) and considerable PCB/on-chip area penalty when implemented separately. A remedial approach under extensive research these days is the design of an integrated filtering divider that ensures dual function of a BPF and PD with comparatively less IL, saving valuable PCB/on-chip real estate and ultimately reducing cost.

In a conventional Wilkinson type PD [1], quarter wavelength ($\lambda_g/4$, where λ_g is the guided wavelength) transformers suffer from inherent narrow bandwidth, large area, and poor skirt around the band of interest. These issues of poor signal selectivity near the design frequency and narrow bandwidth are generally addressed by effectively integrating a BPF in place of $\lambda_g/4$ transformers, resulting in a filtering divider, offering an added advantage of improved out-of-band performance. In addition to achieving the required fractional bandwidth (FBW) with low IL and good input match (low return loss (RL)), a filtering divider must also ensure good output port match and isolation. For this purpose, many types of BPF have been integrated in PDs with different isolation element(s)/techniques employed between the output ports. An ultra-wideband implementation of the

*Correspondence: zafarbedarkhan@mail.nwpu.edu.cn

filtering divider with a resistor and capacitor (RC) as isolation elements was presented in [2]. The achieved output port isolation and RL was 18 dB and 13 dB, respectively. A wide-band filtering divider operational over a FBW of 50% was proposed in [3]. In this work, single-stage coupled lines were employed as BPF in place of conventional $\lambda_g/4$ transformers, achieving miniaturization with resistors as isolation elements. Although for the presented two-way power divider, good size reduction and IL of 3.2 dB were possible, there was still room for improvement in the input and output port matching (S11 and S22/S33) and port isolation, which stood at about 15 dB, 20 dB, and 20 dB, respectively. Filtering dividers with relatively narrower bandwidth (BW) (FBW in the range of 4%–20%) have been reported in [4–10]. In another design approach, coupled-line BPF was integrated in a PD with a 3 dB hybrid used as an isolation element [4]. Here, the port isolation for two presented prototypes was 24 dB each, but the IL was higher at 5.2 dB and 5.4 dB over FBWs of 9.8% and 8.6%, respectively. Other proposals that integrated a couple-line BPF in the PD were presented in [5,6], employing only a resistor as isolation element. Unequal power division was targeted in [5] and equal power division was targeted in [6], and two PD prototypes with integrated second-order and fourth-order coupled-line BPFs, respectively, were implemented. In [5], a good output port isolation of better than 25 dB was achieved, but the IL was as high as 7.4 dB and 9 dB with a 3 dB FBW of 8.7% and 8.6%, respectively, for the two reported prototypes. Similar was the case in [6] where for equal division, a port isolation of about 24 dB was achieved, but the IL for the two prototypes was high at 5.5 dB and 6.8 dB respectively. Here, the achieved 3 dB FBW for the two prototypes was 14.9% and 15.2%, respectively. Quasielliptical BPF was integrated in PD to achieve FBW of 4% in [7]. The presented approach improved the out-of-band rejection but output port isolation (using a resistor as isolation element) was only at 15 dB with high insertion loss of 6.4 dB. Yet another filtering PD design approach used a $\lambda_g/2$ resonator, four $\lambda_g/4$ resonators, and an isolation resistor to achieve an IL of 3.99 dB with output port RL and isolation of 20 dB each [8]. The compact design was operational over a FBW of 6.5%. In this work, the value of the isolation resistor was exceptionally high (3.2 KΩ) to achieve an isolation of 20 dB, deviating considerably from the conventional value. In [9], out-of-band rejection was improved by employing a dual-mode resonator-based BPF in PD to achieve a FBW of 7%. The design employed a resistor of a conventional value of 100 Ω to achieve a port isolation of 16.6 dB and output port RL of 20 dB. Open-loop BPFs were used in [10] and a comprehensive design approach was presented for single- and dual-band filtering dividers. For single-band operation, the design used RL as isolation components to achieve output port RL of 14 dB, port isolation at a center frequency (CF) of about 20 dB (and 37 dB elsewhere in the band). The input port RL and IL was at 18 dB and 3.9 dB, with a reported FBW of 10.1%. From the above discussion, the fact stands out that there is a trade-off between the even-mode response (input port RL and IL) and odd-mode response (output port RL and port isolation) of the filtering divider.

In this paper, a novel technique is presented for achieving good output port isolation and RL while maintaining a reasonably low IL and good input port matching in microstrip implementation of equal-split filtering PD design. In general, a resistor has usually been employed as an isolation element with or without LC components or more resistors in such filtering PD designs to achieve reasonable output port RL and isolation. In this work, in addition to a conventional 100 Ω resistor, an extended transmission line (TL) section of 50 Ω impedance is proposed as isolation element at the output ports for this purpose. In our previous works [11,12], a 50 Ω extended TL section and a 100 Ω resistor were employed in two- and three-transmission–line dual-band Wilkinson power dividers (WPDs) to achieve satisfactory S-parameters employing 2-port cascaded network analysis to calculate circuit parameters. In this work, the concept is extended to the filtering divider design.

However, the main difference here from our previous work is the challenge of effective BPF integration in place of TLs with simultaneous effective port isolation, which calls for a novel analysis approach altogether different from [11,12]. In this work, BPFs are designed first keeping the even/odd mode circuit requirements in mind and subsequently integrated in the PD. Two of the famous candidates among different types of BPFs, namely coupled-line filter (CLF) and open-loop coupled resonator filter (OLF), have been selected and integrated in the PD with the proposed isolation elements for effective output isolation and RL, simultaneously maintaining reasonably low ILs and good input matches. If the BPF is matched to 70.7 Ω, it can effectively replace the conventional $\lambda_g/4$ transformers in a WPD. The two filtering dividers thus designed also provide good out-of-band rejection. Employing the proposed approach for microstrip implementation has an advantage of avoiding lumped reactive elements (capacitor and inductor) and the isolation resistor has a conventional value of 100 Ω, which is easily found in commercially available SMD packages.

2. Proposed methodology for filtering power divider design

The block diagram of the proposed filtering divider circuit with a TL section and an isolation resistor is depicted in Figure 1a. BPFs have been used to replace the conventional $\lambda_g/4$ transformers. It may be noted that to achieve effective output port isolation and RL in dual-band WPD, a 50 Ω extended TL of length l_{TL} and a resistor R were used [11,12]. For the best possible functional response of the filtering PD, l_{TL} and the tapping position of the output ports on the 50 Ω extended TL were optimized (optimization process is explained in detail in the related subsections). Owing to the symmetry of the proposed circuit in Figure 1a, even/odd mode analysis is applicable. Figures 1b and 1c show the respective even-mode and odd-mode half circuits of the proposed filtering PD.

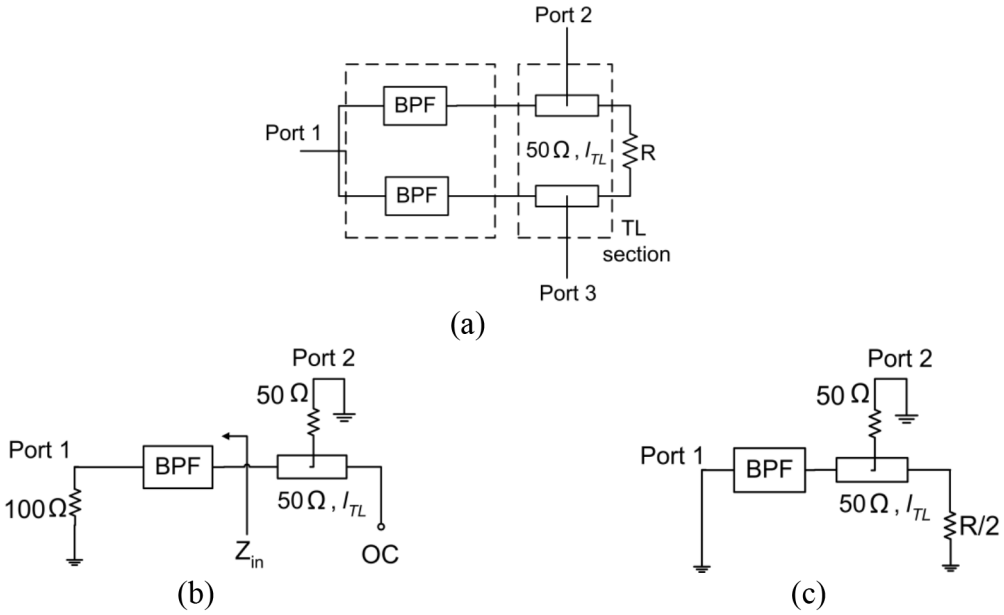

Figure 1. (a) Proposed filtering divider. (b) Even-mode circuit. (c) Odd-mode circuit.

Referring to Figure 1a, when even-mode excitation is applied at the outputs, the symmetric plane becomes an open circuit (magnetic wall) and yields the circuit shown in Figure 1b, where the isolation resistor R becomes superfluous (shown as open circuit). Careful analysis of the even-mode circuit reveals that for output port 2 of

50 Ω, the impedance of input port 1 is 100 Ω. In order to achieve a perfect match of the input port and output port, a transformation of 70.7 Ω is required as in conventional PD design. Now if a BPF is to replace the impedance transformer (which is the case here), it must be matched to 70.7 Ω, so that Z_{in} is equal to 50 Ω, as shown in Figure 1b. This implies that for proper band-pass response, the port settings must be 70.7 Ω instead of 50 Ω while simulating the BPF. Thus, under even-mode conditions, the proposed structure is expected to equally divide the signal with the filtering functionality and maintain good IL and input port match (good RL).

Odd-mode analysis was carried out to ensure good output port isolation and RL. As evident in Figure 1c, under odd-mode excitation at the output ports, the symmetric plane can be replaced by a short circuit (electric wall). If port 2 is perfectly matched, then input port 1 is shorted and no power is transferred, whereas maximum power is delivered to the isolation resistor, which is half of its original value. Thus, for good isolation between output ports 2 and 3 (each 50 Ω), the resistor value was taken to be 100 Ω (R = 2 × 50 Ω). TL and the tapped position of the output port are optimized to achieve good output port RL and isolation. In order to show the efficacy of the proposed technique, two design examples integrating two different types of BPFs in the PD are presented and the results are discussed in the following sections.

3. Design examples

3.1. Coupled line filter divider (CLFD) design

3.1.1. Coupled line filter (CLF)

As stated earlier, many authors have selected coupled lines/coupled-line filters for integration in the PD [3–6], but with tradeoffs between the even- and odd-mode performances. For effective replacement of the conventional $\lambda_g/4$ transformers, an even-ordered filter should be designed [5,6]. As in the first design example, a second-order coupled-line filter with a Chebyshev response, pass-band ripple of 0.1 dB, and FBW of 16% designed at a CF of 3 GHz was selected.

The design procedure of such CLFs is well known [13,14]. For completeness, a brief design description is provided. First of all, the low-pass filter prototype elements for the desired specifications of the CLF were $g_0 = 1$, $g_1 = 0.843$, $g_2 = 0.622$, and $g_3 = 1.355$. Band-pass conversion was carried out by calculating the admittance (J) inverter values from Eq. (1), and subsequently even- and odd-mode impedances by Eq. (2) [13]. Based on these values of even- and odd-mode impedances, widths (w) and distances (d) were calculated for each coupled-line section, as shown in Figure 2a. The band-pass filter was implemented in Agilent's Advance Design System (ADS) software (Santa Clara, CA, USA) and the dimensions were slightly optimized for the required band-pass response. The finalized CLF parameters are summarized in Table 1.

$$\frac{J_{01}}{Y_0} = \sqrt{\frac{\pi FBW}{2g_0g_1}}, \frac{J_{j,j+1}}{Y_0} = \frac{\pi FBW}{2}\frac{1}{\sqrt{g_jg_{j+1}}}(j = 1ton-1), \frac{J_{n,n+1}}{Y_0} = \sqrt{\frac{\pi FBW}{2g_ng_{n+1}}} \quad (1)$$

Table 1. Calculated design parameters of the CLF.

j	$J_{j,j+1}$	$(Z_{0e})_{j,j+1}$	$(Z_{0o})_{j,j+1}$	$w_{j,j+1}$ (mm)	$d_{j,j+1}$ (mm)
0	0.557	132.05	53.25	0.715	0.18
1	0.362	105.5	54.9	1.012	0.24
2	0.557	132.05	53.25	0.715	0.18

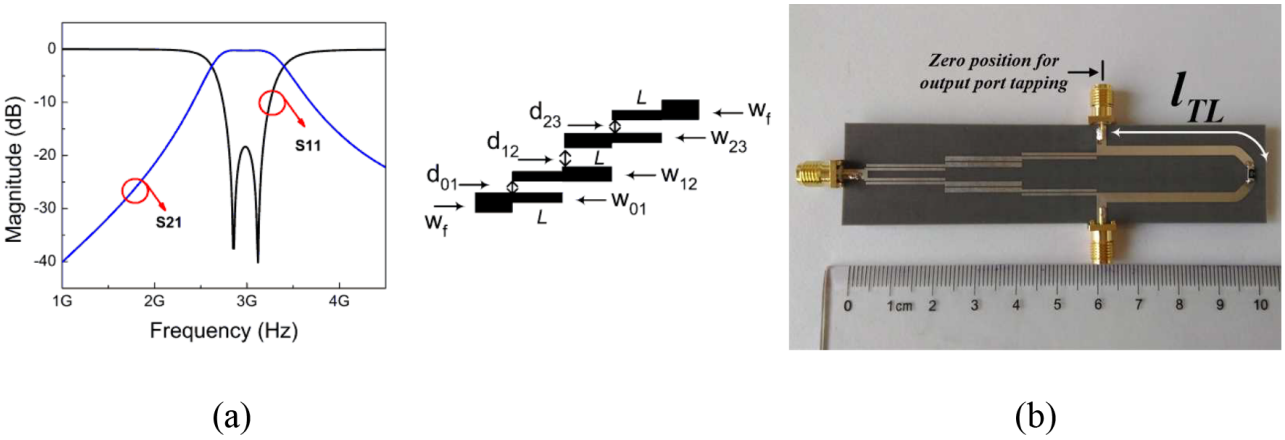

Figure 2. (a) Simulated response of second-order CLF. (b) The manufactured CLFD at 3 GHz.

$$(Z_{0e})_{j,j+1} = \frac{1}{Y_0}\left[1 + \frac{J_{j,j+1}}{Y_0} + \left(\frac{J_{j,j+1}}{Y_0}\right)^2\right], (j = 0ton), (Z_{0o})_{j,j+1} = \frac{1}{Y_0}\left[1 - \frac{J_{j,j+1}}{Y_0} + \left(\frac{J_{j,j+1}}{Y_0}\right)^2\right] \quad (2)$$

where

$J_{j,j+1}$	Admittance (J) inverter parameters
Y_0	Characteristic admittance of the terminating line (with $Z_0 = 70.7\ \Omega$)
FBW	Fractional bandwidth = BW/CF
n	Order of the filter
$(Z_{0e})_{j,j+1}$	Even-mode impedance
$(Z_{0o})_{j,j+1}$	Odd-mode impedance

Please note that for calculation purposes, the system impedance is taken as $Z_0 = 70.7\ \Omega$ to solve Eqs. (1) and (2); subsequently, in simulation, the port is set to 70.7 Ω as well. It may be noted from Figure 2a that the length L of each coupled-line section is kept same at $\lambda_g/4$. Moreover, the width w_f of the feeding TLs at both connecting ends of the CLF is kept at 1.386 mm, corresponding to 70.7 Ω. Figure 2a also shows the simulated S-parameters of the designed filter at 3 GHz, achieving the desired specifications with a 1 dB BW from 2.71 GHz to 3.2 GHz (FBW of 16.3%).

3.1.2. Coupled-line filtering divider (CLFD)

Effective integration of the designed CLF (with system impedance of 70.7 Ω used in Eqs. (1) and (2)) in the PD was carried out by substituting it in place of the conventional $\lambda_g/4$ transformers (Figure 1a) and tapping the output ports initially from the zero position (zero position is taken just where the BPF ends), as shown in Figure 2b. The isolation elements were the proposed TL and a resistor. In order to ensure good even-mode response and subsequent odd-mode response through respective half circuits, l_{TL} and the output port tapping position were tuned in each half circuit. Please note here that the isolation resistor was kept at a conventional value of 100 Ω and only l_{TL} and the tapping position were optimized. Since in each half circuit, different S-parameters were tuned by tuning the aforementioned parameters, an initial optimization range of l_{TL} and the tapping position was determined. Finally, in the full circuit simulation of the CLFD, l_{TL} and the tapping position were optimized in the range of $\lambda_g/8 < l_{TL} < \lambda_g/2$ and 0 to l_{TL}, respectively. For the purpose, the

optimization tool was used in ADS. The optimization goals were set to minimize S22/S33 and S23, with l_{TL} and the port tapping position set as variables. The optimized results were achieved at $l_{TL} = \lambda_g/2 = 37$ mm and output ports tapped from zero position on the l_{TL} (just where the BPF ended). The CLFD was fabricated on a F4BM-2 substrate with a dielectric constant of 2.2 and height of 0.8 mm. Figure 2b shows the fabricated CLFD. The area of the manufactured CLFD came out to be 24.24 cm^2 (10.1 cm $\times$ 2.4 cm, or $1.3\lambda_g \times 0.3\lambda_g$). The size is slightly bigger in one dimension, but as will be shown in the subsequent section, the proposed design simultaneously achieved satisfactory even- and odd-mode response.

3.2. Open-loop coupled resonator filtering divider (OLFD) design

3.2.1. Open-loop coupled resonator filter (OLF)

The design procedure of an OLF is well known [13,15,16]. However, the OLF may be implemented in different shapes, such as square [10,15,16] or triangular [17–19]. As a second design example, a triangular OLF was selected to be integrated in a PD. The design process is presented here for the sake of thoroughness.

A right isosceles triangular implementation of the OLF of second order was carried out at a design frequency of 1 GHz. The open-loop triangular filter (OLTF) was designed for a Chebyshev response with a pass-band ripple f 0.1 dB and a FBW of 10%. The low-pass prototype elements were $g_0 = 1$, $g_1 = 0.843$, $g_2 = 0.622$, and $g_3 = 1.355$. Subsequently, the coupling coefficient (k_{12}) and external quality factor (Qe) were calculated as 0.14 and 8.43, respectively, from Eq. (3).

$$k_{12} = k_{21} = FBW/\sqrt{g_1 g_2},$$

$$Qe = (g_0 g_1)/FBW \tag{3}$$

In order to achieve $k_{12} = 0.14$ and Qe $= 8.43$, the OLTF was simulated with F4BM-2 as a substrate, with a dielectric constant of 2.2 and a height of 0.8 mm. All simulations were carried out in ADS. The length of each triangle in the OLTF was kept at $\lambda_g/2$ [13]. Referring to Figure 3a, it may be noted that the presented structure is symmetrical with dimensions of each right isosceles triangle given as: length of each cathetus (c) = 31.5 mm, hypotenuse (h) = 49 mm, and gap (g) = 3 mm. Moreover, the width (w) was set equal to 2.44 mm. During simulation, for effective integration of the OLTF in the PD, the filter was matched to 70.7 Ω by setting the ports to this value and optimizing. Mixed coupling was employed to achieve the required k by coupling both resonators through their catheti at a suitable separation from each other, whereas Qe was achieved by optimizing the input feed position (d). Separation (s) between the resonators inversely affects k (more s implies less k), while Qe is affected by d, which is greatest at the middle of the resonator and decreases as the feed position is moved away from the center. The split-mode frequencies achieved by synchronously tuned resonators at different s values were used to calculate k, while the 3 dB bandwidth, which varies by optimizing d, was used to obtain Qe, as given in Eq. (4). The optimized values were $s = 1.5$ mm and $d = 11$ mm.

$$k_{12} = (f_1^2 - f_2^2)/(f_1^2 + f_2^2),$$

$$Qe = f_0/\Delta f_{3dB}, \tag{4}$$

where

f_0, f_1, and f_2 = design frequency and lower and higher split frequencies

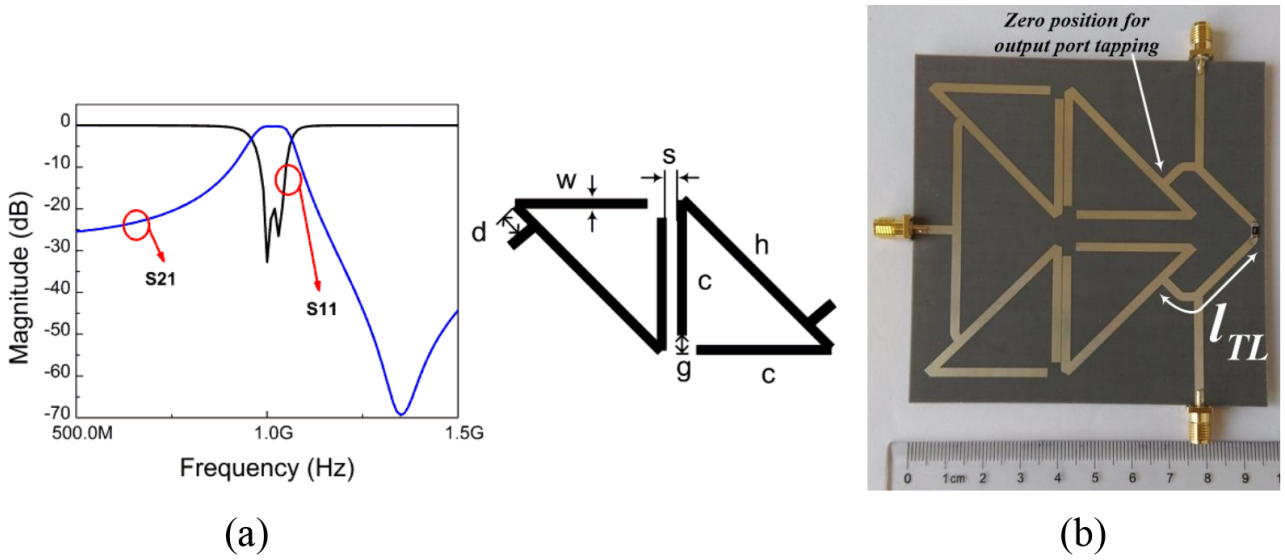

Figure 3. (a) Simulated response of second-order OLTF. (b) The manufactured OLFD at 1 GHz.

Δf_{3dB} = 3 dB bandwidth

A simulated S-parameter response of the designed OLF is also depicted in Figure 3a. A 1 dB BW was achieved from 0.96 GHz to 1.06 GHz (FBW = 10%), with good overall performance.

3.2.2. OLFD

The designed OLTF was integrated in the PD as a BPF (Figure 1a) to work effectively with the proposed technique. To achieve good overall performance of the OLFD, keeping the isolation resistor at the conventional value, the optimization ranges of length l_{TL} and the output port tapping position were determined by the even- and odd-mode half circuits for the respective good responses. As a starting point, the output ports were tapped from the zero position (Figure 3b). Subsequently, in the full circuit simulation of OLFD, the symmetrical structure was optimized for l_{TL} and tapping positions in the range of $\lambda_g/8 < l_{TL} < \lambda_g/2$ and zero to l_{TL} (zero position is taken just where the BPF ends, Figure 3b) respectively. The optimization tool in ADS was utilized to optimize l_{TL} and the tapping position to achieve the optimization goals of minimizing S22/S33 and S23. A good S-parameter response was achieved at $l_{TL} \sim \lambda_g/6 = 35$ mm and output ports tapped at 11 mm from the zero position on the l_{TL}. The finalized design of the OLFD was fabricated on a F4BM-2 substrate with a dielectric constant of 2.2 and height of 0.8 mm. Figure 3b shows the fabricated OLFD. The area of the manufactured OLFD came out to be 88.36 cm^2 (9.4 cm $\times$ 9.4 cm, or $0.43\lambda_g \times 0.43\lambda_g$).

4. Results and discussion

All measurements of the two fabricated prototypes presented in the following subsections were carried out on Agilent's PNA, model no. E8363B.

4.1. CLFD

Functional validity of the proposed technique of the presented CLFD design is evident through the conformance of the experimental and simulated S-parameter results at the design frequency of 3 GHz, as depicted in Figures

4a–4e. Wide-band transmission response of the CLFD is illustrated in Figure 4a, where two transmission zeros are seen. The first spurious pass-band appeared at 8.5 GHz and so up to 8 GHz (which is at $2.67f_0$), an out-of-band rejection of better than 15.8 dB was achieved. Figure 4b displays the transmission response in a narrower band explicitly depicting a fairly overlapping response of measured IL (S21 and S31), indicating good symmetry of the presented circuit. The measured input port RL (S11) is at 25 dB, implying a good match, while the insertion loss (S21 and S31) is 3.45 dB (ideal value is 3 dB for equal division). From Figure 4c, it is clear that the output ports (S22 and S33) have RLs of 29 dB each, manifesting good matches. Measured output port isolation (another very important performance parameter ensuring sufficient isolation between the output ports) is 31 dB, as shown in Figure 4d. It may be noted here that port isolation is better at a frequency other than the design frequency of 3 GHz. Since the isolation depends upon the output port return loss, this phenomenon may be explained from the analytical formula for output port isolation given in literature [20,21] as $S23 = (S22_e - S22_o) / 2$ (where subscript "e" and "o" stand for even and odd mode, respectively). In the process of making S23 equal to zero by adjusting isolation parameters in the odd half circuit to match $S22_o$ to $S22_e$ (thus satisfying the given equation for S23), S23 may maximize at frequencies other than the design frequency, since the even- and odd-mode output port RL of the two half circuits may be different. The designed CLFD is operational over a 1 dB BW from 2.71 GHz to 3.17 GHz (1 dB FBW of 15.3%). It may be noted that by employing the proposed technique, good even- and odd-mode responses are achieved simultaneously. Last but not least, Figure 4e shows the measured amplitude imbalance/difference ($|S21| - |S31|$) and phase imbalance/difference ($\angle S21 - \angle S31$) at the output ports of the CLFD over the achieved operational FBW. It is clear that at the design frequency of 3 GHz, the amplitude difference is 0.036 dB and phase difference is -0.59°, which implies the presence of a divided signal with almost the same amplitude and phase at the output ports.

4.2. OLFD

In a similar fashion as above, the operation of the second design example (OLFD) was experimentally validated. Figures 5a–5e present the comparison of the simulated and measured S-parameters. An overall good conformance can be observed. Figure 5a illustrates the wide-band transmission response of the OLFD, indicating good out-of-band-performance. Here, the first spurious pass-band appeared at 3.1 GHz. An out-of-band rejection of better than 16 dB was achieved up to 2.85 GHz ($2.85f_0$). A narrow-band view of the transmission characteristics is given in Figure 5b. A reasonable match at the input port with input RL (S11) of 24 dB was achieved. Moreover, a symmetric (almost overlapping) response of insertion loss (S21 and S31) is also evident with a value of 4.2 dB at 1 GHz (CF). Figure 5c depicts the output port RL of S22 = S33 = 32 dB, implying a good match with reasonable overlapping response. Isolation between the output ports was 20 dB, as demonstrated in Figure 5d. Here, too, the isolation was greatest at a frequency different from the design frequency due the reasoning given in Section 4.1. Figure 5e illustrates that at the design frequency of 1 GHz, the magnitude difference and phase difference at the output ports are 0.2 dB and -2°, respectively, which is reasonably acceptable. The operational 1 dB BW ranges from 0.92 GHz to 1.04 GHz (1 dB FBW of 12%).

4.3. Comparison of the proposed methodology with previous work

A comparison of the presented work with some previous works is presented in Table 2.

In the comparison table, it can be seen that references [4–7] present very high IL while maintaining reasonable input/output port RL and isolation. On the other hand, [8–10] have good IL, but with some

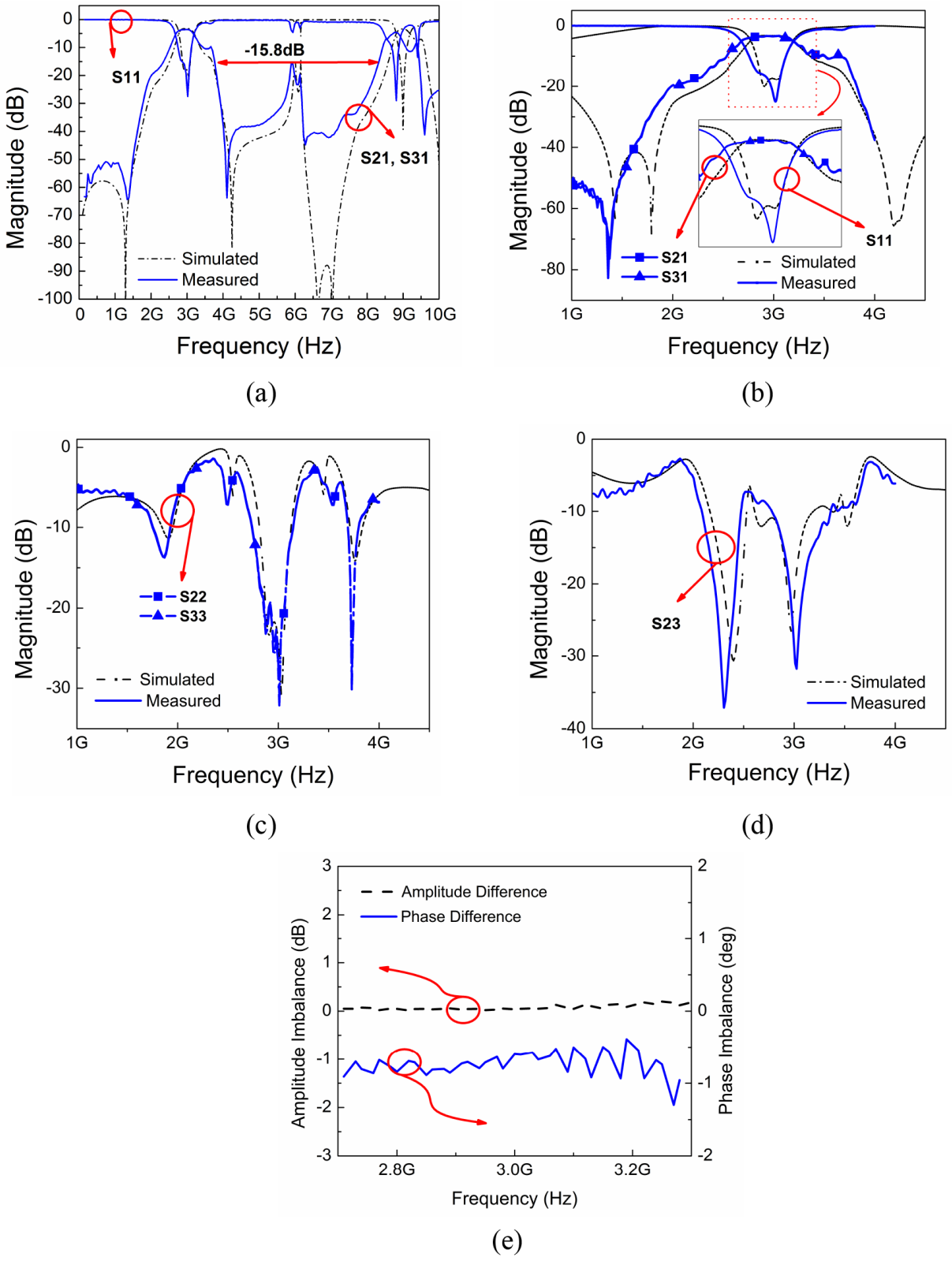

Figure 4. Measured versus simulation response of CLFD. (a) Wide-band response. (b) Transmission characteristics in narrow band. (c) Output port return loss. (d) Output port isolation. (e) Amplitude and phase imbalance at output port.

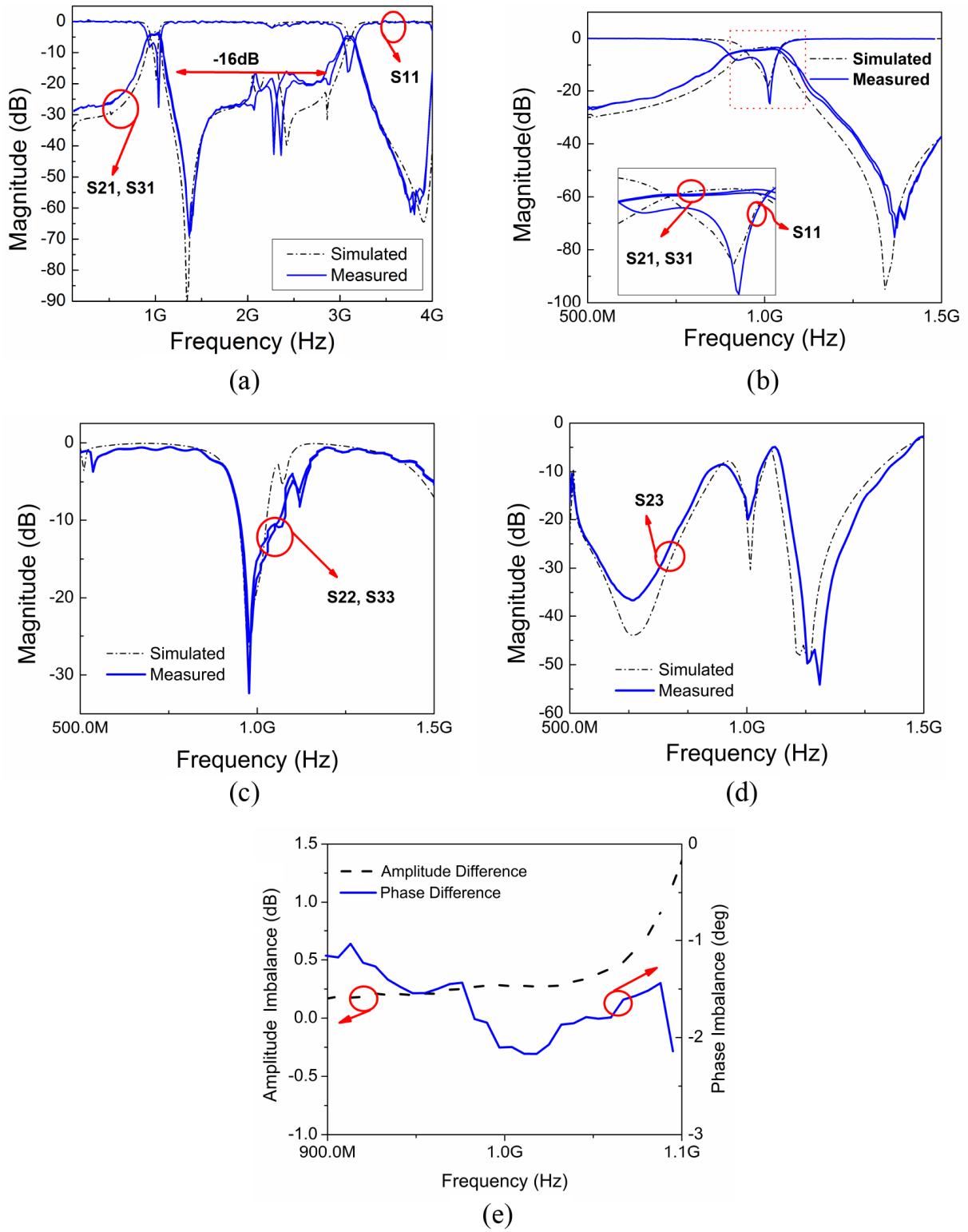

Figure 5. Measured versus simulation response of OLFD. (a) Wide-band response. (b) Transmission characteristics in narrow band. (c) Output port return loss. (d) Output port isolation. (e) Amplitude and phase imbalance at output port.

Table 2. Comparison of proposed work with previous work.

Works		Parameters							
		n*	BPF Type	Iso** elements	Input RL dB	IL dB	Output RL dB	Iso** dB	FBW (%)
[4]		5	Coupled line filter	3dB Hybrid	30	5.2	30	25	9.8
[5]		2	Coupled line filter	R	25	8	25	31	7.5
		4	Coupled line filter	R	> 25	9.9	> 25	32	7.3
[6]		2	Coupled line filter	R	27	5.5	27	24	14.9
		4	Coupled line filter	R	25	6.8	25	24	15.2
[7]		4	Quasi-elliptical filter	R	~ 25	6.4	~ 25	15	4
[8]		3	Quasi-elliptical filter	R	20	3.99	20	20	6.5
[9]		2	Dual-mode resonator	R	24	~ 4.2	20	16.6	7
[10][a]		2	Open-loop resonator	RL	~ 18	3.9	14	~ 20	10.1
This work	CLFD	2	Coupled line filter	TL, R	25	3.45	29	31	15.3
	OLFD	2	Open-loop resonator	TL, R	24	4.2	32	20	12

[a]Only single-band filtering divider was taken from this reference.

*Order of the filter.

**Isolation.

compromise on the RL and isolation. The presented two design examples (CLFD and OLFD with a TL and resistor as isolation elements) achieved reasonable values for all S-parameters. It is worth mentioning that although the OLFD, when compared to its own class of single-band open loop filtering divider presented in [10], had a slightly higher IL (0.3 dB more), the output port RL improved to 32 dB in contrast to a marginal increase of 14 dB in [10]. It may therefore be concluded that for band-limited filtering dividers (FBW from 4% to 20%), the presented methodology achieved good even- and odd-mode responses simultaneously.

5. Conclusion

A novel methodology has been presented for designing a filtering divider with a transmission line and resistor as isolation elements. It was proven that by employing the proposed technique, good simultaneous even-mode and odd-mode responses could be achieved. The filtering divider design challenges were unique and different from that of a PD design (employing the transmission line and resistor as isolation elements presented in [11,12]), which were successfully addressed. First, a CLF and OLF were matched to 70.7 Ω in the simulation and then integrated in the PD with a 50 Ω extended TL and a 100 Ω resistor as isolation elements. The designed CLFD and OLFD were fabricated and shown to be operational over a FBW of 15.3% and 12% at design frequencies of 3 GHz and 1 GHz, respectively. Moreover, a sufficiently wide out-of-band response was achieved for most practical purposes. The achieved S-parameters (S11, S22/S33, S21/S31, S23) in both the design examples were reasonably good, validating the proposed idea.

References

[1] Pozar DM. Microwave Engineering. 2nd ed. New York, NY, USA: Wiley, 2009.

[2] Xiao L, Peng H, Yang T. A novel power divider integrated with one bandpass filter. Progress in Electromagnetics Research C 2014; 52: 115-124.

[3] Singh PK, Basu S, Wang YH. Coupled line power divider with compact size and bandpass response. Electron Lett 2009; 45: 892-894.

[4] Llorent-Romano S, Garcia-Lamperez A, Salazar-Palma M, Daganzo-Eusebiot AI, Galaz-Villasantet JS, Padill-Cruzin MJ. Microstrip filter and power divider with improved out-of-band rejection for a Ku-band input multiplexer. In: 33rd European Microwave Conference; 7 October 2003; Munich, Germany. pp. 315-318.

[5] Deng PH, Dai LC. Unequal Wilkinson power dividers with favourable selectivity and high-isolation using coupled-line filter transformers. IEEE T Microw Theory 2012; 60: 1520-1529.

[6] Deng PH, Dai LC, Chen YD. Integrating equal-split Wilkinson power dividers and coupled-line bandpass filters. In: Electromagnetics Research Symposium Proceedings; 19–23 August 2012; Moscow, Russia. pp. 1249-1253.

[7] Shao JY, Huang SC, Pang YH. Wilkinson power divider incorporating quasi-elliptical filters for improved out-of-band rejection. Electron Lett 2011; 47: 1288-1289.

[8] Zhang XY, Wang KX, Hu BJ. Compact filtering power divider with enhanced second-harmonic suppression. IEEE Microw Wirel Co 2013; 23: 483-485.

[9] Song K. Compact filtering power divider with high frequency selectivity and wide stopband using embedded dual-mode resonator. Electron Lett 2015; 51: 495-497.

[10] Li YC, Xue Q, Zhang XY. Single- and dual-band power divider integrated with bandpass filters. IEEE T Microw Theory 2013; 61: 69-76.

[11] Khan, ZB, Zhao H, Zhang Y. Simplified approach for design of dual-band Wilkinson power divider with three transmission line sections. Microw Opt Techn Let 2016; 58: 2374-2377.

[12] Khan ZB, Zhao H, Zhang Y. A new simplified approach for design of dual-band Wilkinson power divider with two and three transmission line sections using only even-mode analysis. J Microw Optoelectron Electromagn Appl 2016; 15: 390-401.

[13] Hong JS. Microstrip Filters for RF/Microwave Applications. 2nd ed. Hoboken, NJ, USA: Wiley, 2011.

[14] Matthaei GL, Young L, Jones EMT. Microwave Filters, Impedance-Matching Networks and Coupling Structures. New York, NY, USA: McGraw-Hill, 1980.

[15] Hong JS, Lancaster MJ. Couplings of microstrip square open-loop resonators for cross-coupled planar microwave filters. IEEE T Microw Theory 1996; 44: 2099-2109.

[16] Hong JS, Lancaster MJ. Theory and experiment of novel microstrip slow-wave open-loop resonator filters. IEEE T Microw Theory 1997; 45: 2358-2365.

[17] Chaimool S, Kerdsumang S, Akkaraekthalin P. A novel microstrip bandpass filter using triangular open-loop resonators. In: IEEE 9th Asia-Pacific Conference on Communications; 21–24 September 2003; Penang, Malaysia. New York, NY, USA: IEEE. pp. 788-791.

[18] Nedelchev MV, Iliev IG. Synthesis of microstrip filters using triangular open-loop resonators. In: IEEE International Scientific Conference on Information Communication and Energy Systems and Technologies; 23–26 June 2010; Ohrid, Macedonia. New York, NY, USA: IEEE. pp. 141-144.

[19] Hedayati M, Kazemi MJ, Safian R. Design and implementation of a multi triangular microstrip resonator passband filter based on mixed coupling. In: IEEE International RF and Microwave Conference; 12–14 December 2011; Seremban, Malaysia. New York, NY, USA: IEEE. pp. 141-144.

[20] Gao L, Zhang XY, Xue Q. Compact tunable filtering power divider with constant absolute bandwidth. IEEE T Microw Theory 2015; 63: 3505-3513.

[21] Zhao XL, Gao L, Zhang XY, Xu KX. Novel filtering power divider with wide stopband using discriminating coupling. IEEE Microw Wirel Co 2016; 26: 580-582.